

Supplementary Information

Facile synthesis of lead-tin nanoparticles for electrocatalyzing carbon dioxide reduction to formate

Qilong Wang^a, Yayu Guan^a, Jiaying Yan^a, Fanghua Ning^a, Jin Yi^a, and Yuyu Liu^{a,*}

^a Institute for Sustainable Energy/College of Sciences, Shanghai University, Shangda Road 99, Baoshan, Shanghai 200444, China.

*Corresponding authors E-mail addresses: liuyuyu@shu.edu.cn (Y.Y. Liu).

Experimental Section

Chemicals and Materials

Lead nitrate ($\text{Pb}(\text{NO}_3)_2$), Potassium bicarbonate (KHCO_3), Sodium borohydride (NaBH_4), and Nafion solutions (5 wt%) were purchased from Sinopharm Chemical Reagent (Shanghai, China). Stannous chloride (SnCl_2) and Isopropanol ($\text{C}_3\text{H}_8\text{O}$) were obtained from Aladdin (Shanghai, China). Each analytical reagent was directly used without further purification and all aqueous solutions were prepared in deionized water.

Preparation of Catalysts and Electrodes

Catalysts were prepared as follows. First, 7 mL of $\text{Pb}(\text{NO}_3)_2$ (0.1M) solution was added to 40 mL of NaBH_4 (0.1M) solution with vigorous stirring, followed by slowly adding 5 mL of SnCl_2 (0.02M) solution and stirring for 5 minutes. The suspension was then centrifuged at 900 rpm/min, and the solid product was collected and washed several times with deionized water and 95% ethanol. The obtained material was vacuum-dried at 60 °C for 10 hours, and the final product was named Pb_7Sn_1 . In a similar manner, catalysts with other molar ratios were prepared. The prepared Pb and Sn were physically mixed according to molar ratio 7:1, and the obtained catalyst was named Pb_7Sn_1 -1 as the control. Electrodes were prepared as follows. First, the catalyst was ground in mortar for 5 min, then 8 mg of catalyst was mixed with 1 ml isopropanol and 40 μl Nafion solution, dispersed by ultrasonic for 20 min, and finally uniformly spread on $2 \times 2 \text{ cm}^2$ carbon paper (CP).

Physical and Chemical Characterization

The crystal structures of Pb-Sn catalysts were characterized by XRD using an X-ray diffractometer (RIGAKU 3 KW D/MAX-2200V PC, Japan) equipped with a Cu-K α radiation source operated at a scan rate of 8° min⁻¹. XPS was performed using a Thermo Scientific KAlpha apparatus (U.S.A) equipped with a monochromatic Al K α X-ray source to analyze the surface chemical composition and element valence state of the catalysts. The ratio of Pb to Sn was determined by an inductively coupled plasma optical emission spectroscopy (ICP-OES, Agilent 5110). The surface morphology and micro-structures were observed using a scanning

electron microscope (SEM, ZEISS Gemini 300) and a transmission electron microscope (TEM, FEI Tecnai G2 F20) equipped with an EDS. Nitrogen adsorption and desorption measurements were carried out by a Quanta chrome ASAP 2020 M nitrogen adsorption instrument (U.S.A) to obtain the Brunauer-Emmett-Teller (BET) surface area and pore size distribution.

Electrochemical Measurements

All electrochemical experiments to study the electrochemical performance of the Pb-Sn series catalysts were performed on an H-type electrolytic cell connected to an electrochemical workstation (Shanghai Chenhua Instruments Co., Ltd., China). In the conventional three-electrode system, the working electrode (WE) was the as-prepared Pb-Sn catalyst, and the Pt wire and Ag/AgCl (saturated KCl) electrodes were used as the counter electrode (CE) and reference electrode (RE), respectively. The electrolyte was KHCO_3 (0.5 M, 50 mL) and Nafion® 117 film (Dupont, USA) was used to separate the cathodic and anodic compartments. Before measurement, the electrolyte was bubbled with Ar (99.999%) for at least 20 min and then saturated with CO_2 (99.99%) until saturated. The ECR performance of the catalysts were investigated by various electrochemical experiments, such as CV, LSV, electrochemically active surface area (ECSA), and electrochemical impedance spectroscopy (EIS). During the measurement, the flow rate of CO_2 pumping into the cathode chamber was maintained at 160 mL min^{-1} to ensure that the electrolyte remained CO_2 saturated at ambient pressure and temperature. The concentrations of formate and gas products in cathode cell were quantitatively measured by an ion chromatograph (IC1820, Shanghai Sunny Hengping Scientific Instrument Co. Ltd., China) and gas chromatograph (GC-2014C, Shimadzu analytical technology research and a development (Shanghai) Co. Ltd., China), respectively. The calculation formula of FE is given as follows:

$$FE_{\text{Product}} = \frac{E \cdot n \cdot F}{Q_{\text{total}}} \times 100\%$$

Where Q_{total} is the total of electric during electrolysis; E represents the number of electrons required, which is 2 for electrochemical CO_2 reduction and hydrogen evolution here; n is the mol amount of product (formate or H_2), mol; F denotes the Faraday constant (96485 C mol^{-1}).

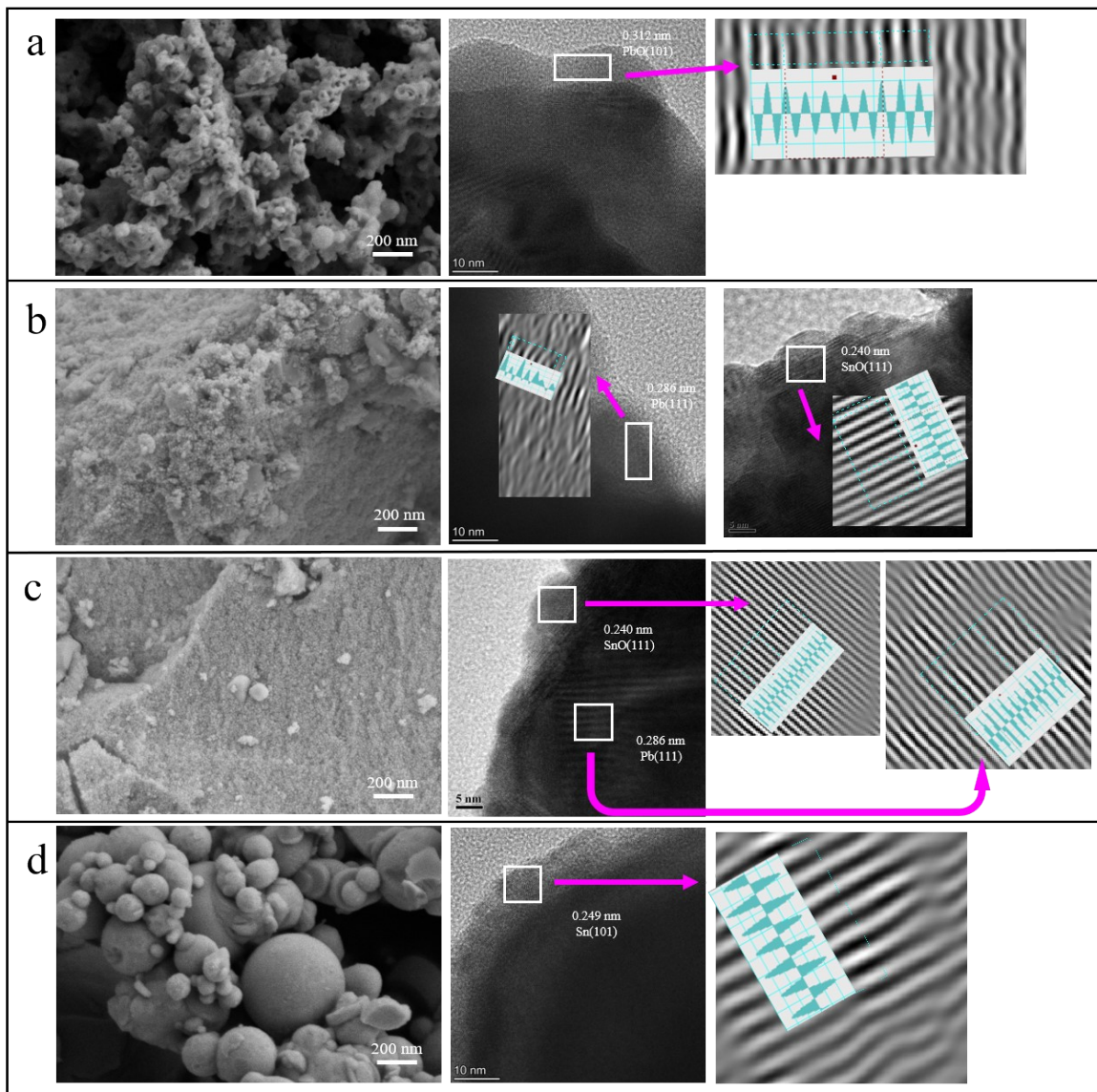


Fig. S1 SEM images and TEM images of (a) Pb, (b) Pb_5Sn_1 , (c) Pb_3Sn_1 and (d) Sn.

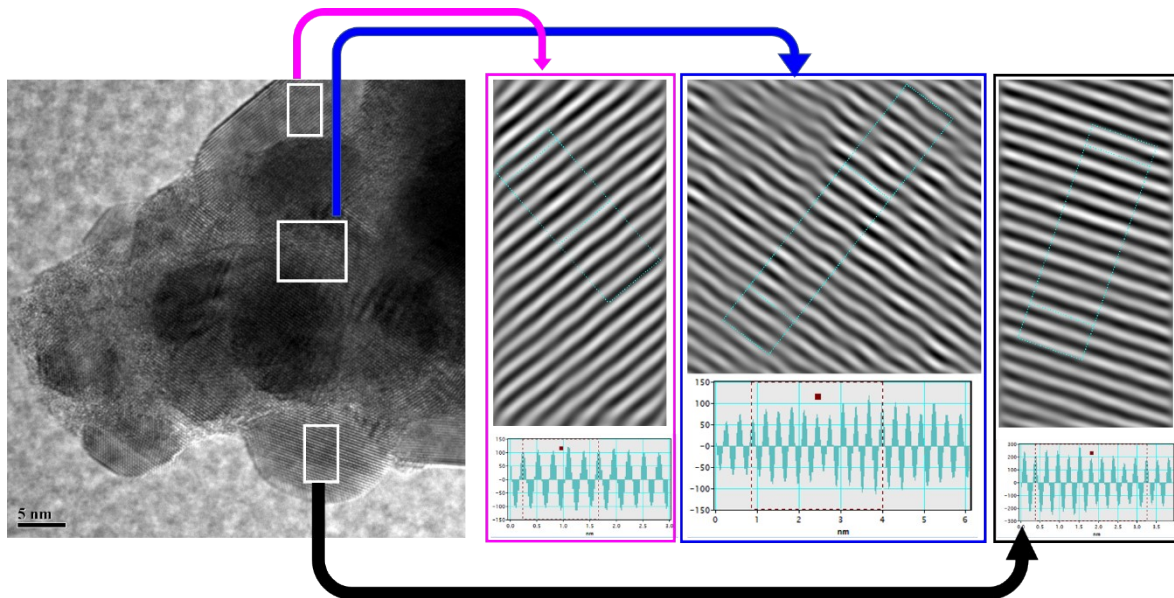


Fig. S2 Optimized HRTEM of Pb_7Sn_1 .

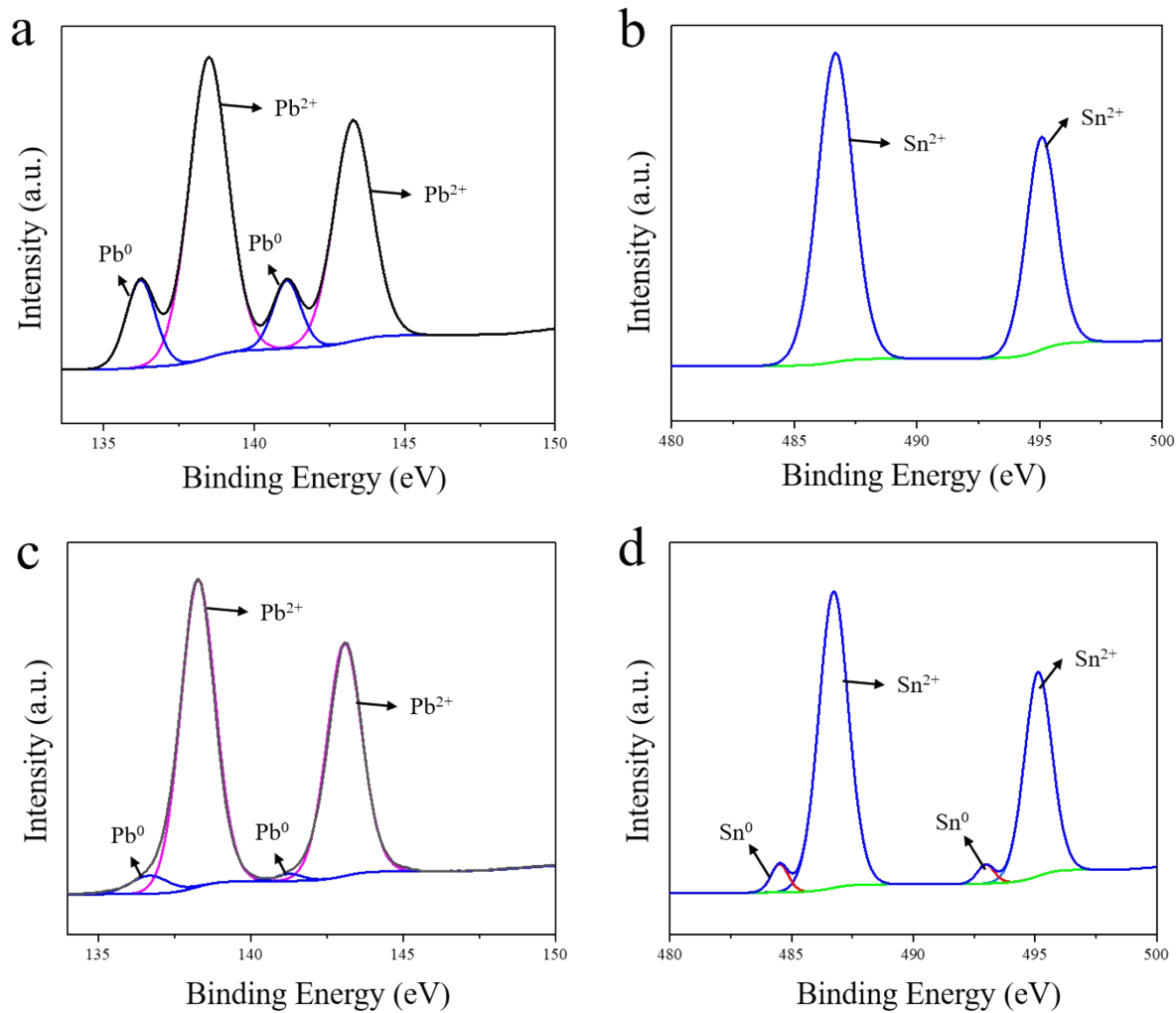


Fig. S3 XPS spectra of Pb_7Sn_1 catalyst: (a) Pb 4f spectrum; (b) Sn 3d spectrum. (c) Pb 4f spectrum of Pb catalyst and (d) Sn 3d spectrum of Sn catalyst.

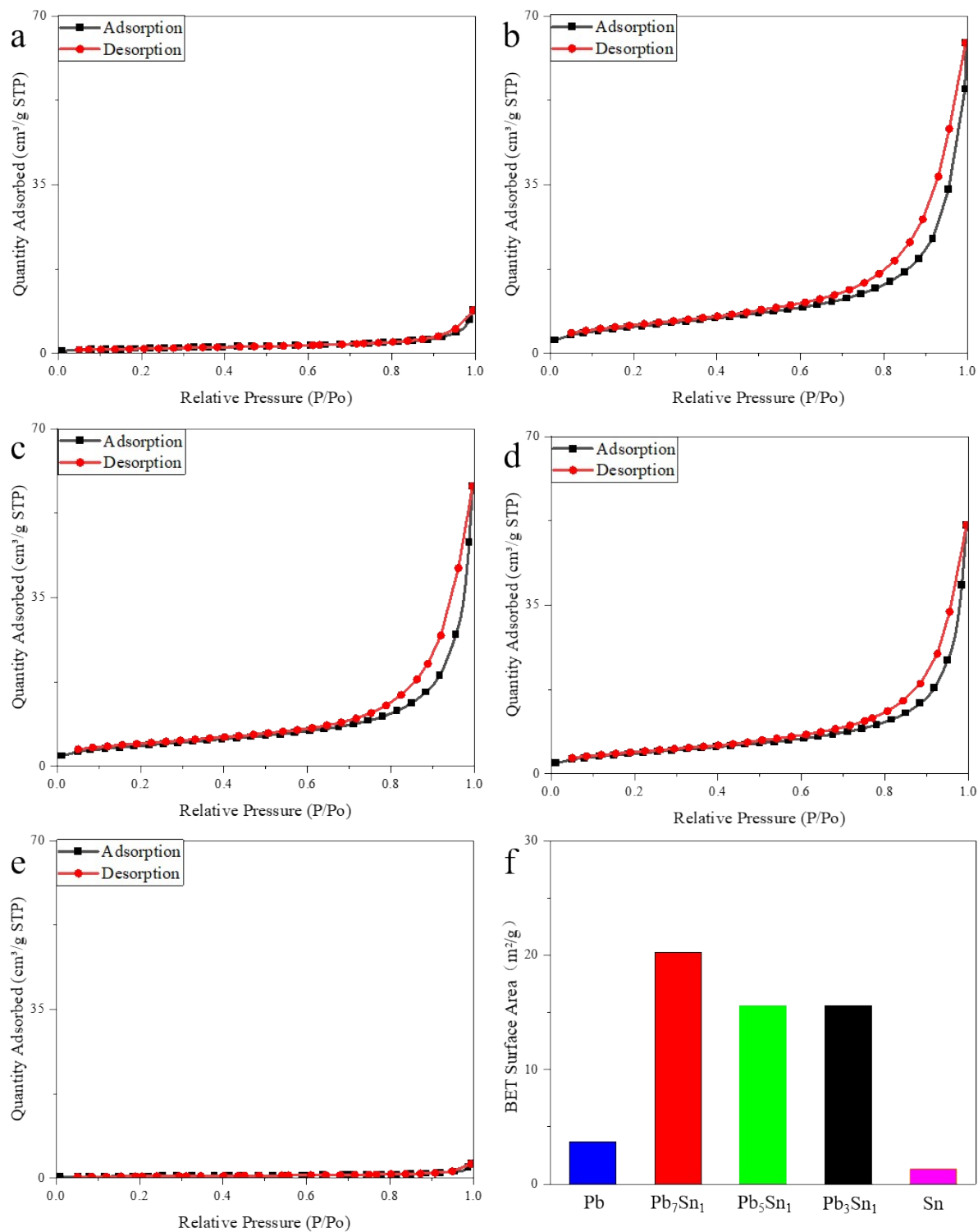


Fig. S4 Nitrogen adsorption-desorption isotherms for (a) Pb, (b) Pb_7Sn_1 , (c) Pb_5Sn_1 , (d) Pb_3Sn_1 and (e) Sn catalysts, and (f) BET surface area of the five catalysts.

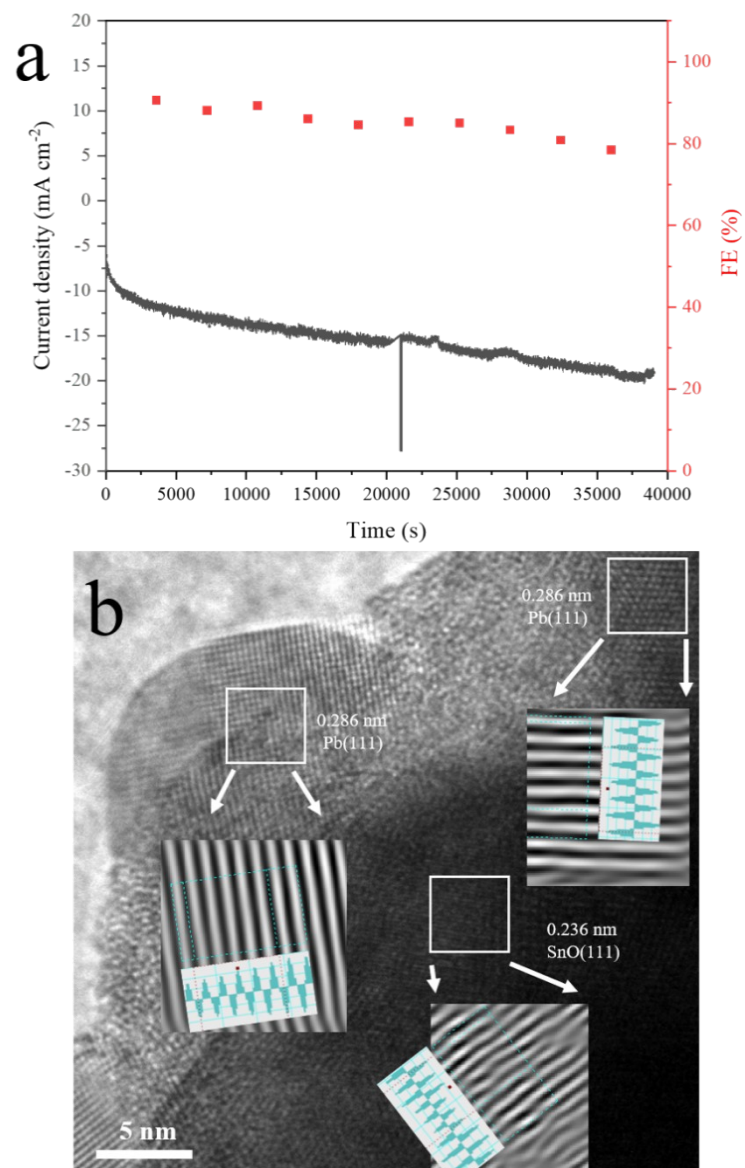


Fig. S5 (a) Pb_7Sn_1 catalyst stability test, and current density and $\text{FE}_{\text{formate}}$ versus time curves; (b) The TEM after stability test of Pb_7Sn_1 .

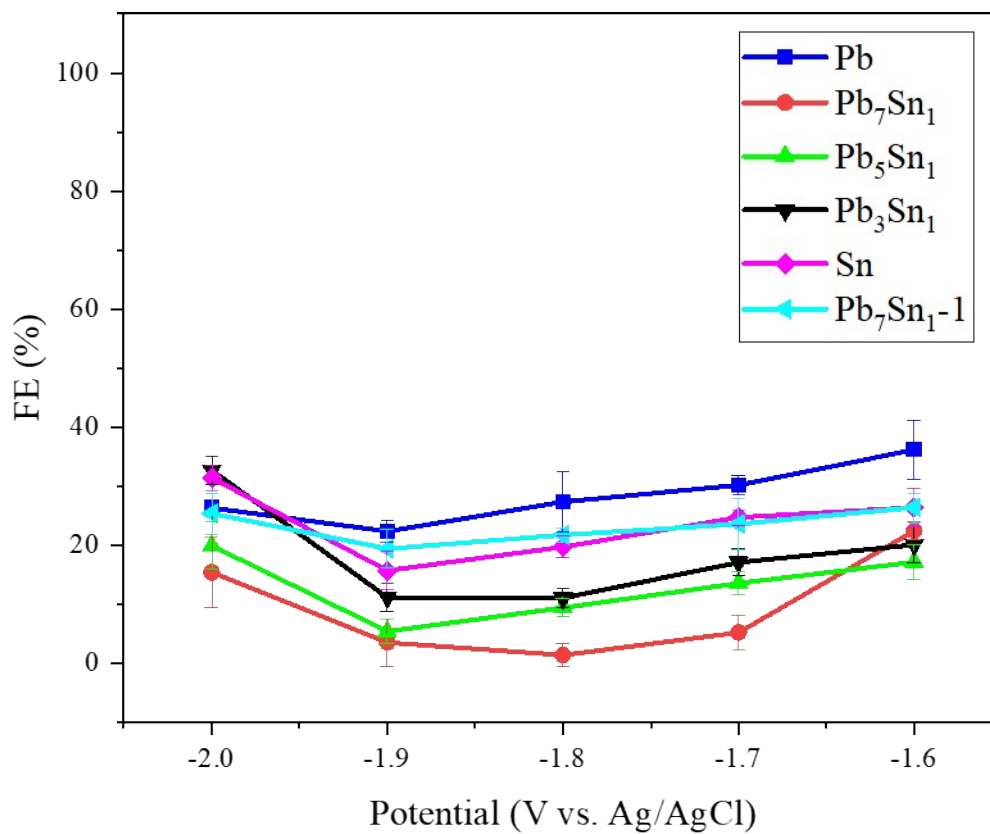


Fig. S6 FE_{H_2} with controlled electrolysis carried out for 30 min on Pb, Sn, and Pb-Sn catalysts.

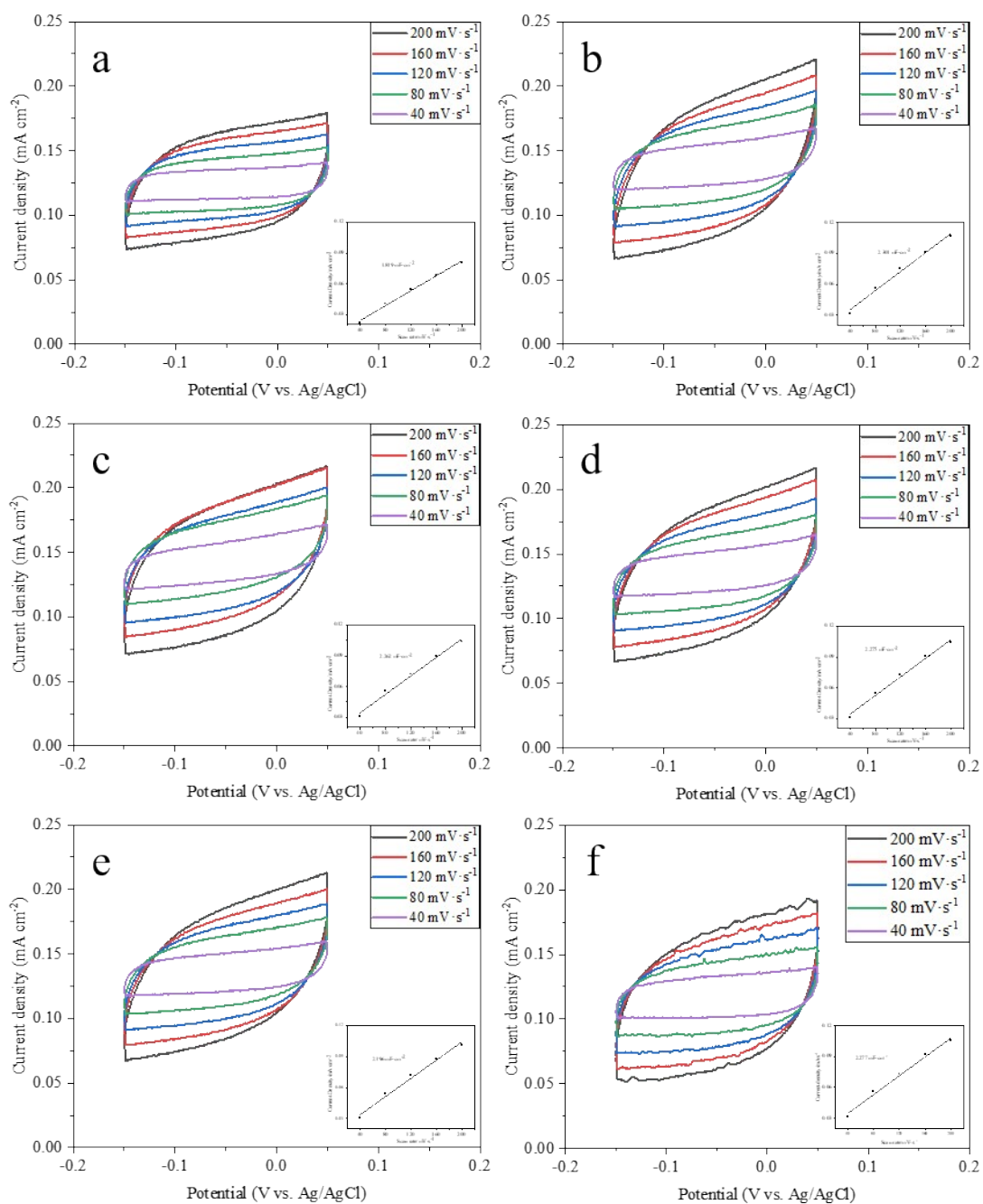


Fig. S7 CV curves of (a) Pb, (b) Pb₇Sn₁, (c) Pb₅Sn₁, (d) Pb₃Sn₁, (e) Sn and (f) Pb₇Sn₁-1 catalysts in Ar-saturated 0.5 M KHCO₃ solution, respectively.

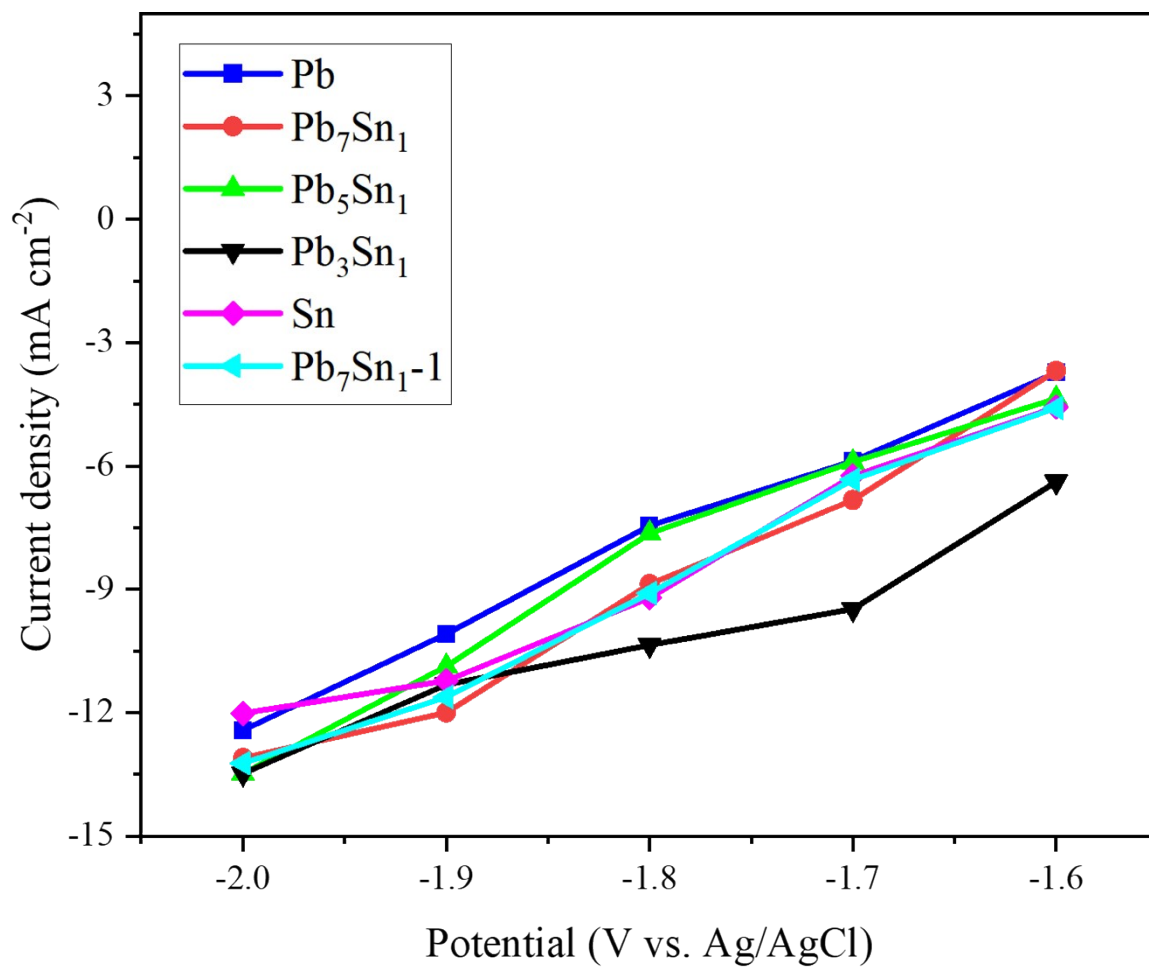


Fig. S8 J_{formate} of Pb, Pb_7Sn_1 , Pb_5Sn_1 , Pb_3Sn_1 , Sn and Pb_7Sn_1-1 catalysts.

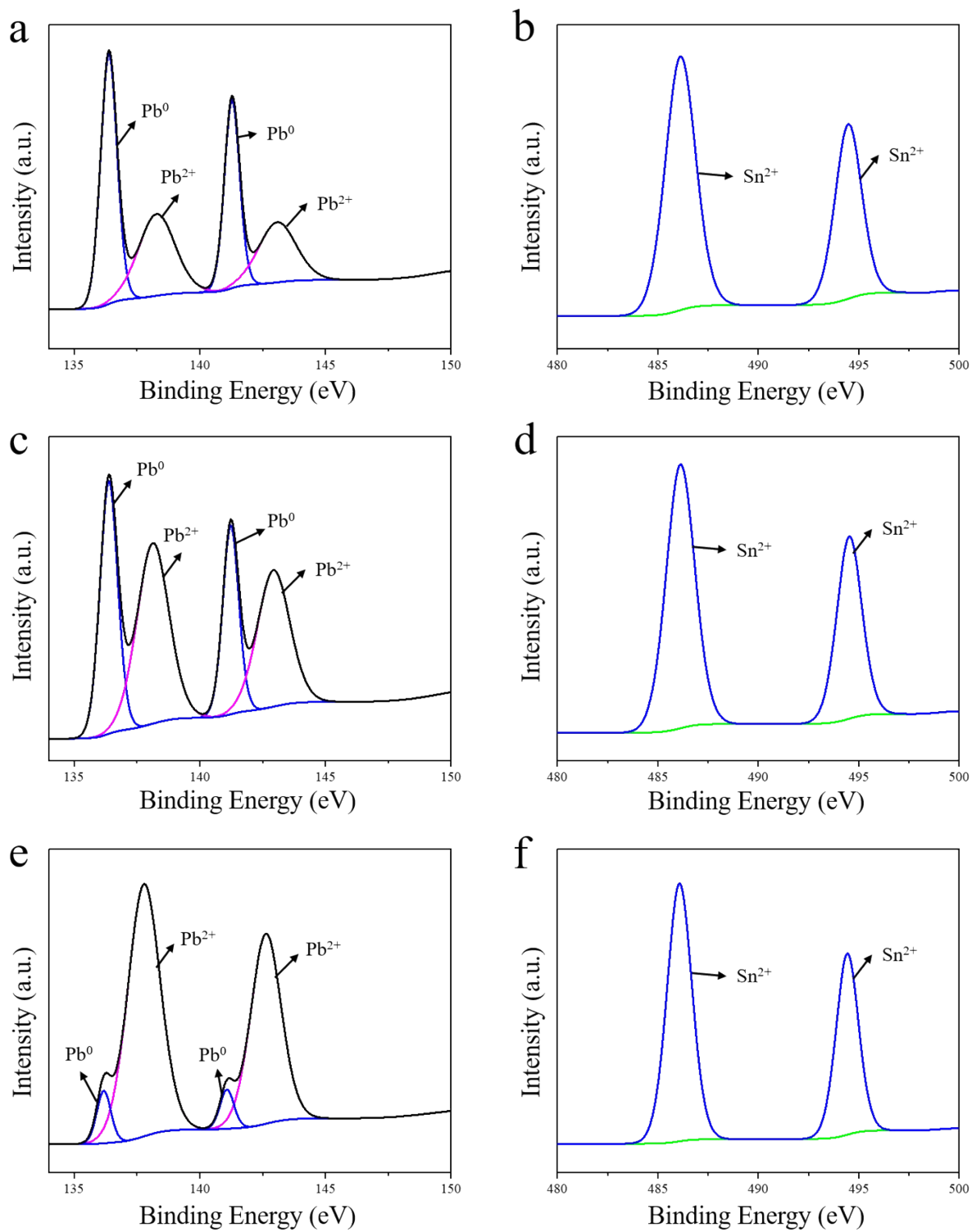


Fig. S9 The XPS of Pb-Sn catalyst after ECR test. (a), (b) Pb₃Sn₁; (c), (d) Pb₅Sn₁; and (e), (f) Pb₇Sn₁.

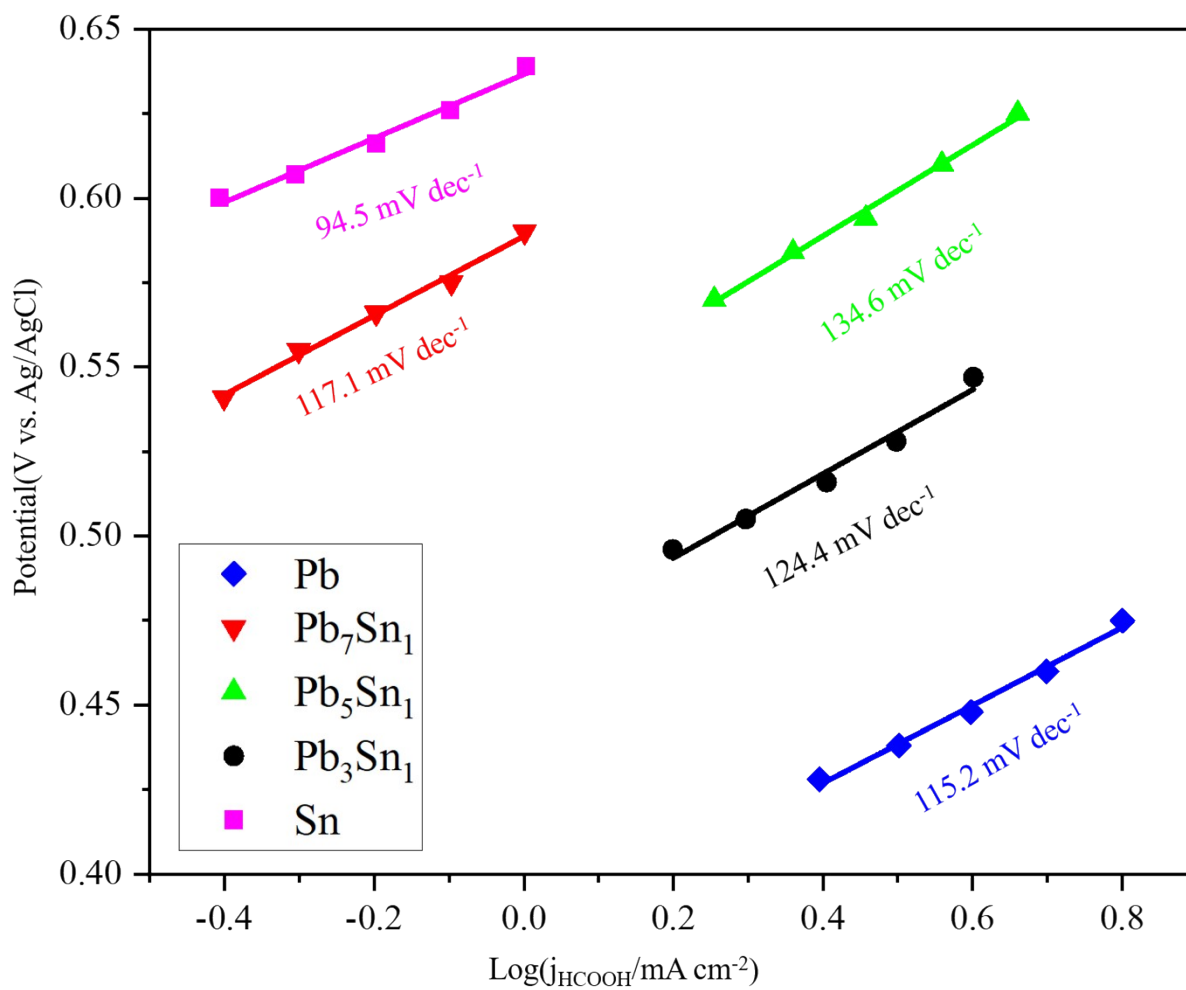


Fig. S10 Tafel plots for formate production on prepared catalyst in CO₂-saturated 0.5 M KHCO₃ solution.

Table S1. ICP results of Pb-Sn catalysts with different compositions.

| | Catalysts | Nominal (mole ratio, Pb/Sn) | ICP-OES (mole ratio, Pb/Sn) |
|-----------------|---------------------------------|--------------------------------|--------------------------------|
| Before ECR test | Pb ₃ Sn ₁ | 3.00 | 2.90 |
| | Pb ₅ Sn ₁ | 5.00 | 4.96 |
| | Pb ₇ Sn ₁ | 7.00 | 6.95 |
| After ECR test | Pb ₃ Sn ₁ | 3.00 | 2.78 |
| | Pb ₅ Sn ₁ | 5.00 | 5.13 |
| | Pb ₇ Sn ₁ | 7.00 | 7.1 |

Table 2. Comparison of recently reported catalyst performance

| Electrocatalyst | Electrolyte Composition | Potential | FE(%) | j(mA cm ⁻²) | Ref. |
|--|--|-----------------------|---|-------------------------|------|
| Pb(111) | a mixture of 0.1 mol·L ⁻¹ HNO ₃ and 0.01 mol L ⁻¹ NaF in aqueous solution | -0.83 V (vs. RHE) | 98.03(HCOO ⁻) | ~2.4 | 1 |
| PbPd bimetallic catalyst | 0.5 M HCOOK | -1.5 V (vs. Ag/AgCl) | ~85(HCOO ⁻) | 5.6 | 2 |
| Pb | 0.5 M NaOH | -1.6 V (vs. SCE) | 90(HCOO ⁻) | 2.5 | 3 |
| PbZn bimetallic catalyst | 0.1 M KHCO ₃ | -1.2 V (vs. RHE) | 95(HCOO ⁻) | 47 | 4 |
| PbSnO ₃ /C | 0.1 mol L ⁻¹ tetrabutylammonium hexafluorophosphate in propylene carbonate solution. | -1.9 V (vs. Ag/AgCl) | 85.1(oxalate) | 2 | 5 |
| Pb ₁ Cu | 0.5 M KHCO ₃ | -0.8 V (vs. RHE) | 96(HCOO ⁻) | 800 (Flow cell) | 6 |
| PbSn bimetallic catalyst | 0.5 M KHCO ₃ | -2.0 V (vs. Ag/AgCl) | 79.8(HCOO ⁻) | 45.7 | 7 |
| PbSn bimetallic catalyst | an IL/acetonitrile/water electrolyte | -1.95 V (vs. Ag/AgCl) | 91±3(HCOO ⁻) | 7.7±0.2 | 8 |
| Pb/Au | 0.5 M KHCO ₃ | -1.07 V (vs. RHE) | ~25% (CO) ~40% (H ₂) ~25% (HCOO ⁻) 2.8% (CH ₄) | 0.33 | 9 |
| Pd-doped Pb ₃ (CO ₃) ₂ (OH) ₂ | 0.1 M KHCO ₃ | -1.20 V (vs. RHE) | 96.5% (HCOO ⁻) | 13 | 10 |
| oxide-derived Sn-Pb-Sb alloy | 0.1 M KHCO ₃ | -1.4 V (vs. RHE) | 91% (HCOO ⁻) | 8.3 | 11 |
| CuPb bimetallic catalyst | 0.1 M KHCO ₃ | -1.3 V (vs. RHE) | 73.5%(C ₂ + products) | 294.4 | 12 |
| CuPb bimetallic catalyst | 0.5 M KHCO ₃ | -0.93 V (vs. RHE) | 29.6% (CO) 35.6% (H ₂) 9.2% (HCOO ⁻) | 9.35 | 13 |
| BiPb bimetallic electrode | 0.5 M KHCO ₃ | -0.96 V (vs. RHE) | 91.86%(HCOO ⁻) | 15.56 | 14 |
| Sn on Cu nanowires | 0.1 M KHCO ₃ | -1.2 V (vs. RHE) | 86.8(HCOO ⁻) | 38.0 | 15 |

| | | | | | |
|----------------------------------|-------------------------|----------------------|----------------------------|-------|-----------|
| Sn-modified ZIF-based composites | 0.5 M KHCO ₃ | -1.16 V (vs. RHE) | 76.70(HCOO ⁻) | 9.81 | 16 |
| Sn-NOC | 0.1 M KHCO ₃ | -0.7 V (vs. RHE) | 94(CO) | 14.81 | 17 |
| Bi/Sn bimetallic | 0.1 M KHCO ₃ | -1.0 V (vs. RHE) | 94.80(HCOO ⁻) | 34.0 | 18 |
| Pb-Sn catalyst | 0.5 M KHCO ₃ | -1.9 V (vs. Ag/AgCl) | 90.53%(HCOO ⁻) | 12.3 | This work |

References

1. W. Yu, L. Wen, J. Gao, S. Chen, Z. He, D. Wang, Y. Shen and S. Song, *Chem Commun (Camb)*, 2021, **57**, 7418-7421.
2. X. Lu, Y. Wu, X. Yuan and H. Wang, *Angew Chem Int Ed Engl*, 2019, **58**, 4031-4035.
3. B. Innocent, D. Liaigre, D. Pasquier, F. Ropital, J. M. Léger and K. B. Kokoh, *Journal of Applied Electrochemistry*, 2008, **39**, 227-232.
4. A. G. A. Mohamed, E. Zhou, Z. Zeng, J. Xie, D. Gao and Y. Wang, *Adv Sci (Weinh)*, 2022, **9**, e2104138.
5. Y. Cheng, P. Hou, H. Pan, H. Shi and P. Kang, *Applied Catalysis B: Environmental*, 2020, **272**.
6. T. Zheng, C. Liu, C. Guo, M. Zhang, X. Li, Q. Jiang, W. Xue, H. Li, A. Li, C. W. Pao, J. Xiao, C. Xia and J. Zeng, *Nat Nanotechnol*, 2021, **16**, 1386-1393.
7. S. Y. Choi, S. K. Jeong, H. J. Kim, I.-H. Baek and K. T. Park, *ACS Sustainable Chemistry & Engineering*, 2016, **4**, 1311-1318.
8. A. Hailu, A. A. Tamijani, S. E. Mason and S. K. Shaw, *Energ Fuel*, 2020, **34**, 3467-3476.
9. A. M. Ismail, G. F. Samu, H. C. Nguyen, E. Csapo, N. Lopez and C. Janaky, *ACS Catal*, 2020, **10**, 5681-5690.
10. W. Huang, Y. Wang, J. Liu, Y. Wang, D. Liu, J. Dong, N. Jia, L. Yang, C. Liu, Z. Liu, B. Liu and Q. Yan, *Small*, 2022, **18**, e2107885.
11. S. Rasul, A. Pugniant, H. Xiang, J.-M. Fontmorin and E. H. Yu, *Journal of CO2 Utilization*, 2019, **32**, 1-10.
12. P. Wang, H. Yang, Y. Xu, X. Huang, J. Wang, M. Zhong, T. Cheng and Q. Shao, *ACS Nano*, 2021, **15**, 1039-1047.
13. Y. Wang, H. Hu, Y. Sun, Y. Tang, L. Dai, Q. Hu, A. Fisher and X. J. Yang, *Advanced Materials Interfaces*, 2019, **6**.
14. X. Zhang, X. Jiao, Y. Mao, X. Zhu, H. Kang, Z. Song, X. Yan, X. Yan, C. Han, L. Cui, K. Zhang and J. Qiao, *Separation and Purification Technology*, 2022, **300**.
15. G. Chen, D. Ye, R. Chen, J. Li, X. Zhu and Q. Liao, *Journal of CO2 Utilization*, 2021, **44**.
16. Y. Guan, Y. Liu, J. Yi and J. Zhang, *Dalton Trans*, 2022, **51**, 7274-7283.
17. J. Guo, W. Zhang, L. H. Zhang, D. Chen, J. Zhan, X. Wang, N. R. Shiju and F. Yu, *Advanced Science*, 2021, **8**.
18. Z. Li, Y. Feng, Y. Li, X. Chen, N. Li, W. He and J. Liu, *Chem Eng J*, 2022, **428**.